

ABSTRACT

We present the results of the analysis of stellar flares based on TESS observations. We used the two-minute cadence data obtained from sectors 1-37. Our software allows us to identify flares and determine its basic parameters such as: amplitude, duration, growth and decay times. We estimate the total energy of flares in two different methods. We investigate distributions of flare frequencies and its dependence upon spectral types. We already identified about 130 000 flares from more than 23 000 flaring stars from F-type to M-type. From the analysis we conclude that approximately 7.5% of all observed stars show flaring activity, which is in agreement with other papers on this topic. Based on bolometric flare energy estimations, we conclude that its energies range from 10^{31} to 10^{36} erg, with an average energy of 10^{33} erg. The result of the performed analysis is also the statistical distribution of the parameters of flaring stars.

INTRODUCTION

Stellar flares are rapid events, occur during magnetic reconnection in the stellar corona. Stored magnetic energy is impulsively released, converted and consequently radiated across the entire electromagnetic spectrum. TESS is a space-based telescope, which provides continuous observation of about 85% stars from all the celestial sphere, therefore it is perfect for detecting stellar flares.

RESULTS

We identified about 130 000 flares from more than 23 000 flaring stars. The most common flare activity was shown by stars of the spectral type M (about 40%). The star with the biggest number of detected flares (more than 700) is TIC150359500 observed in 22 sectors.

The Figure 1 shows the distributions of the basic parameters of stellar flares: amplitudes, growth and decay times. The most of amplitudes do not exceed the value of 0.2 of the normalized flux with subtracted background. The duration of a stellar flares ranges from a few minutes to several hours and the maximum of the flares duration distribution is approximately 30-40 minutes. The average values of the growth times are much shorter than the decay times and are usually below 20 minutes. The decay time distribution have maximum about 30 minutes.

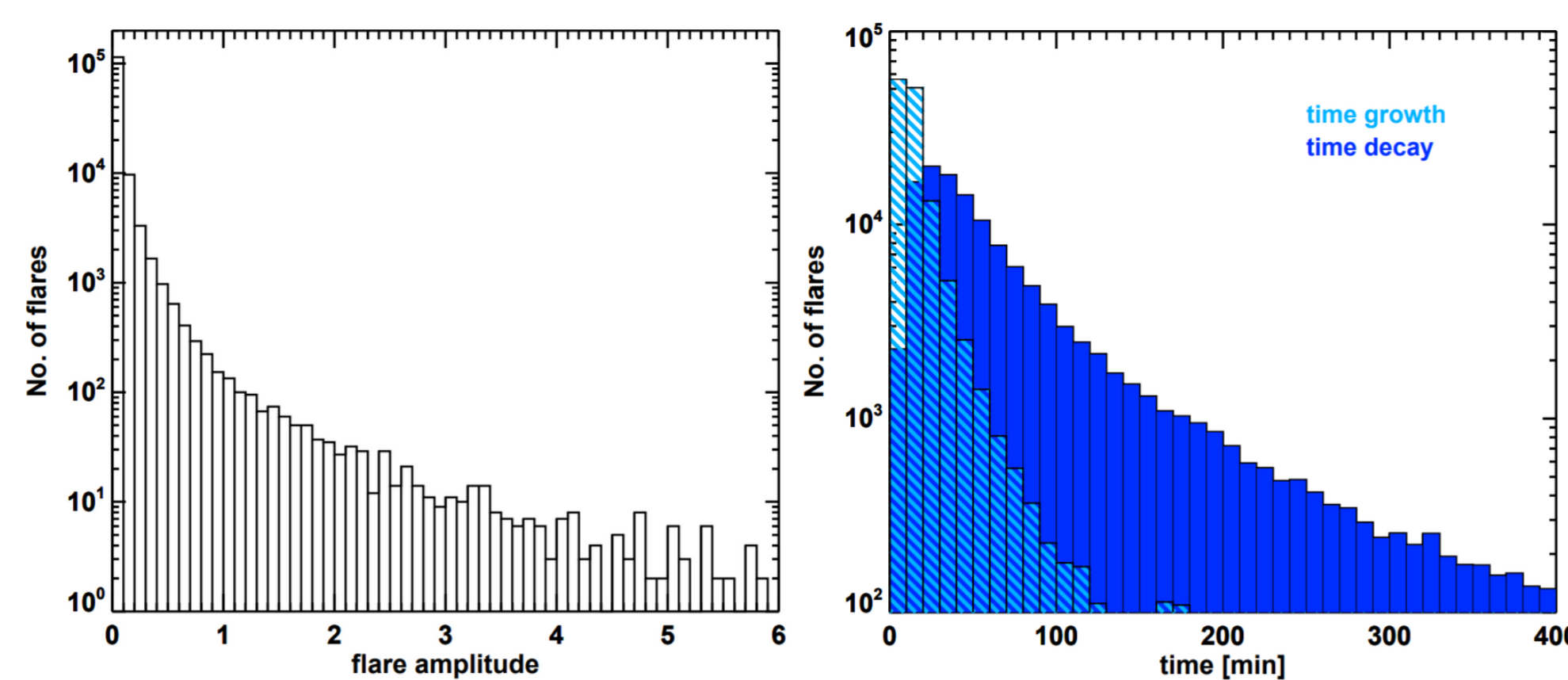


Figure 1: The distributions of the basic parameters of stellar flares: amplitude, growth and decay times.

The Figure 2 shows some of the distributions of the basic parameters of flaring stars: effective temperatures and spectral types. All analyzed stars are marked in gray, and flaring stars are marked in dark blue. Most flaring stars are cool stars, with temperatures up to 4000 K (spectral type M). There is also a less significant group of flares on stars at temperatures up to about 8000 K, which corresponds to the spectral types F, G and K. Only stars below the F0 spectral type are analyzed.

METHODS OF FLARES DETECTION

For finding flares from TESS (The Transiting Exoplanet Survey Satellite) data we prepared an automated, three step software WARPfinder (Wrocław AlgoRithm Prepared For detectiNg and analysing stEllar flares). The first step is trend method based on consecutive de-trending of the light curves. Then we determine the standard deviation and check which data points protrude above the assumed sigma level. These detections are saved as potential stellar flares. This idea was taken from a paper by Davenport et al. (2014). The second step is the difference method. It is based on checking the flux difference between two consecutive points and examining the standard deviation. We define all points with a value greater than 3σ as a potential flare detection. The difference method was inspired by Shibayama et al. (2013). The events times of both methods are compared and the prepared list of potential stellar flares are then verified by the third method. We fit the assumed flare profiles to the observational data and check its quality with chi-square statistic. To distinguish a stellar flare from data noise we use the probability density function of F-distribution. Additional methods to reject false detections are the calculation of the flare profile skewness and the sector method. Moreover, we assume that a stellar flare should have a shorter rise time than its decline. We also reject all events with a duration of less than 6 observational points (12 minutes).

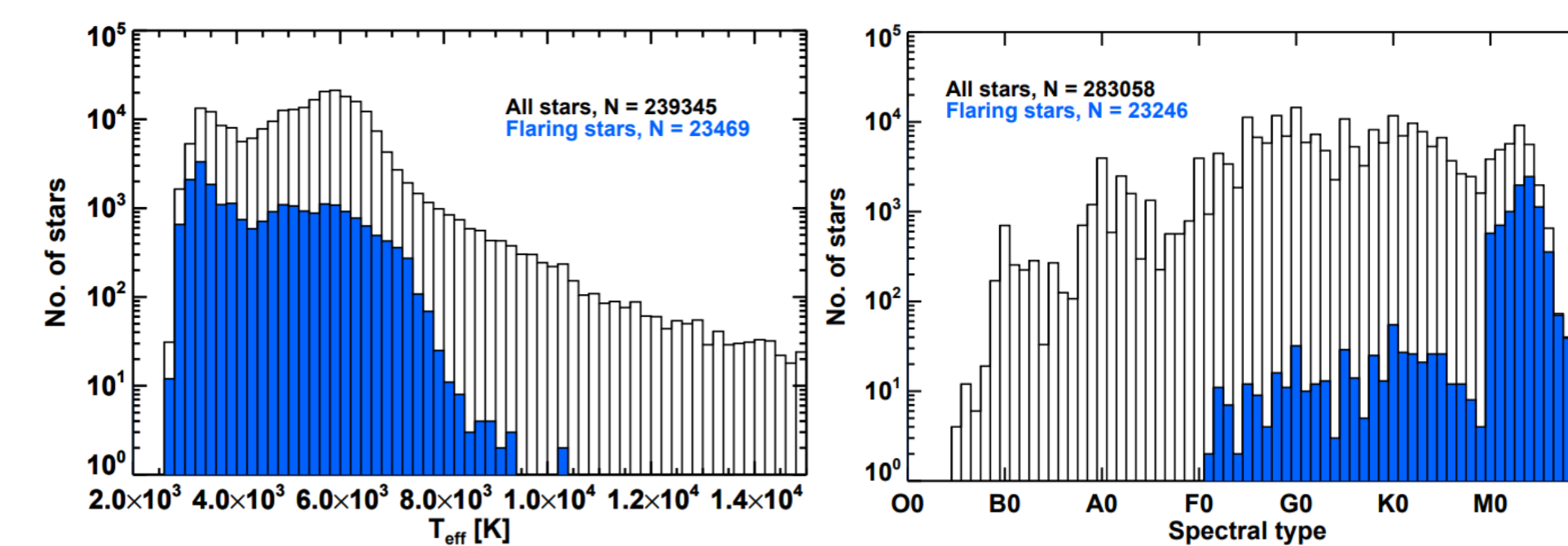


Figure 2: Histograms of the number of flaring stars (dark blue) compared with the total number of stars shown as a function of the stellar effective temperature and spectral type.

We compare our results with works such as Feinstein et al. (2020) and Doyle et al. (2020). Figure 3 shows the histograms of the total number of stars from sectors 01-20 and the number of flaring stars from our analysis and from Feinstein et al. (2020) shown as a function of the stellar effective temperature. The distributions agree with each other very well. On Figure 4 we compare the distributions of spectral types within flaring stars observed in sectors 01-13 from our work and from Doyle et al. (2020). A different distribution of the spectral types may result from the methods of searching for flares.

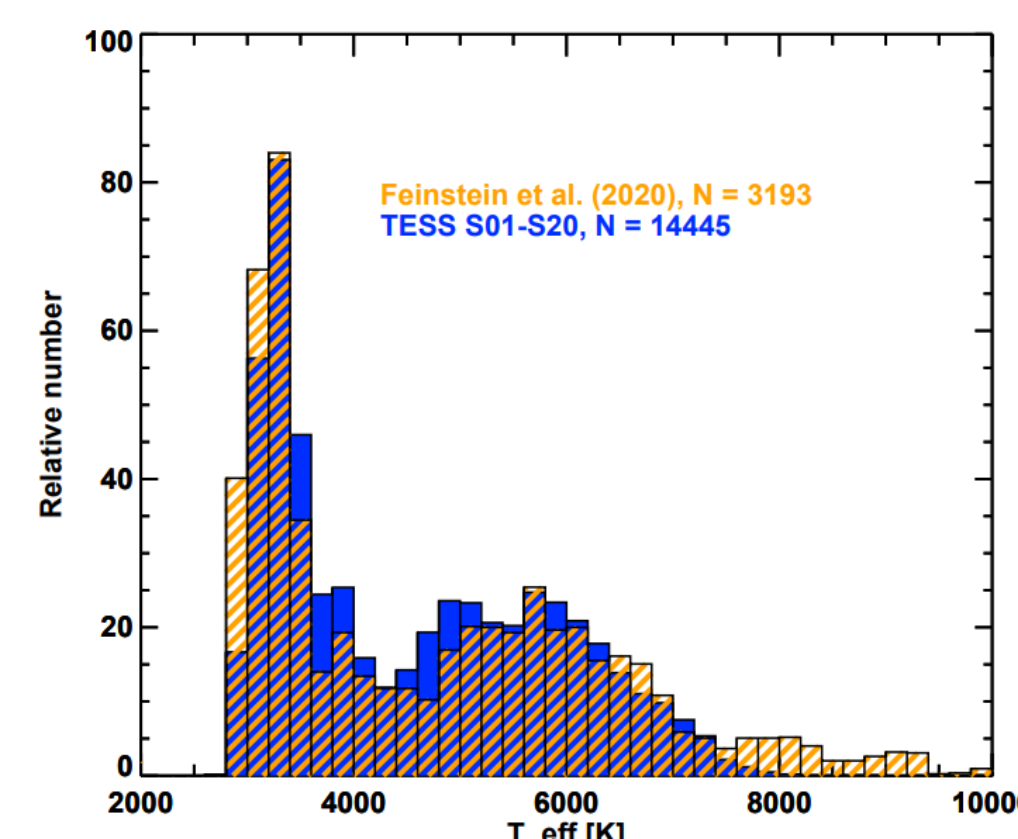


Figure 3: Histograms of flaring stars effective temperature (S01-S20). Comparison of our results (dark blue) and Feinstein et al. (2020) (orange).

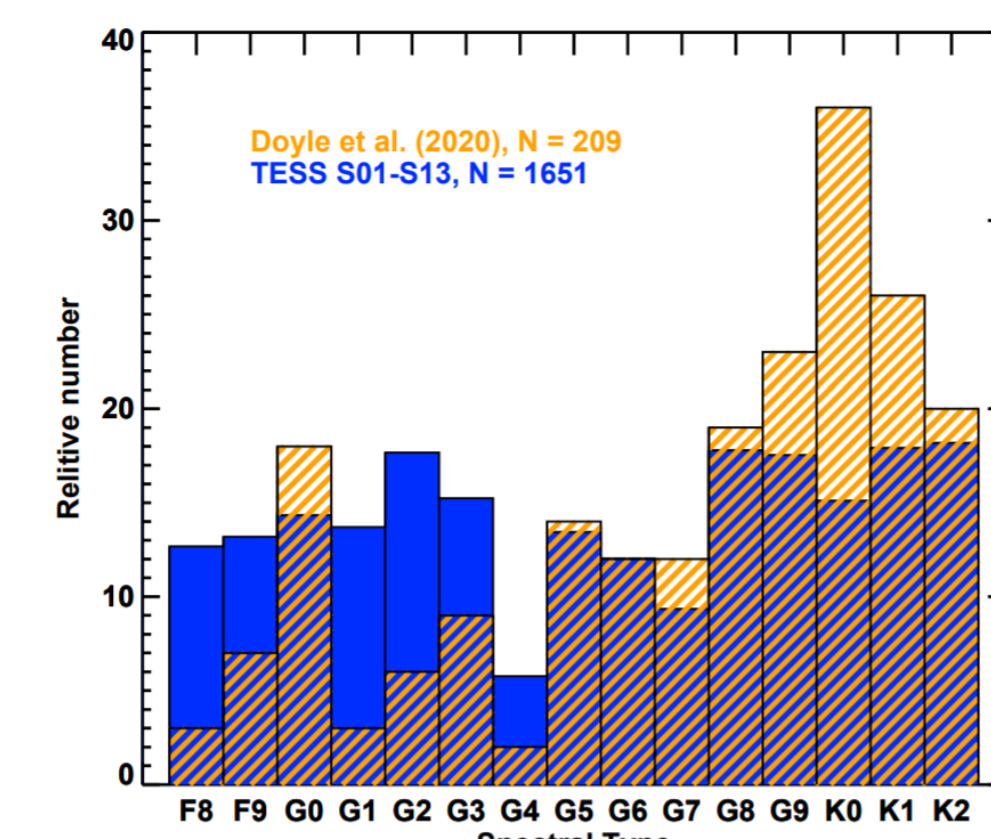


Figure 4: Histograms of flaring stars spectral type (S01-S13). Comparison of our results (dark blue) and Doyle et al. (2020) (orange).

FLARE ENERGIES

Our software estimates the maximum luminosity and total energy of flares in two different methods. In the first one we assume black body radiation and effective temperature of a flare (T_{flare}) about 10000 K (Mochnacki Zirin (1980); Hawley Fisher (1992); Shibayama et al. (2013)). The bolometric flare luminosity (L_{flare}) and energy (E_{flare}) could then be calculated from:

$$L_{flare} = \sigma_{SB} T_{flare}^4 A_{flare} \quad (1)$$

$$E_{flare} = \int_{t1}^{t2} L_{flare}(t) dt \quad (2)$$

The flare area (A_{flare}) is a function of flare amplitude, stellar radius, TESS response function and Planck function.

The second one is the method proposed by Kovari et al. (2007). In the first step we estimate the relative flare energy ϵ_{TESS} by integrating the normalized flare intensity I_{norm} during the flare event:

$$\epsilon_{TESS} = \int_{t1}^{t2} I_{norm} dt \quad (3)$$

Then we calculate flux of the star F_{star} using the spectrum of star $F(\lambda)$ taken from ATLAS9 (Castelli & Kurucz (2003)). Stellar radius R , $\log(g)$, T_{eff} and TESS response function $S_{TESS}(\lambda)$ are required in this method:

$$F_{star} = \int_{\lambda_1}^{\lambda_2} 4\pi R^2 F(\lambda) S_{TESS}(\lambda) d\lambda \quad (4)$$

Finally we estimate the flare energy E_{flare} from stars flux F_{star} in selected interval of wavelengths and relative flare energy ϵ_{TESS} :

$$E_{flare} = F_{star} \cdot \epsilon_{TESS} \quad (5)$$

The Figure 5 shows the histograms of flare energies from our analysis. Energy calculated using method based on Shibayama et al. (2013) is marked in dark blue and based on Kovari et al. (2007) with light blue. The results of both methods differ from each other by a factor of 4. The method using the spectrum of star usually gives higher energy estimation. In every case energies of stellar flares ranges from 10^{31} to 10^{36} erg, with an average about 10^{33} erg. It is in agreement with previous papers on this topic (Lacy et al. (1976), Hawley et al. (2014), Maehara et al. (2020)). Figure 6 shows the distributions of the flare energies from our sample of stars from sectors S01-S02 and from Gunther et al. (2020) (colored orange). The distributions generally agree with each other.

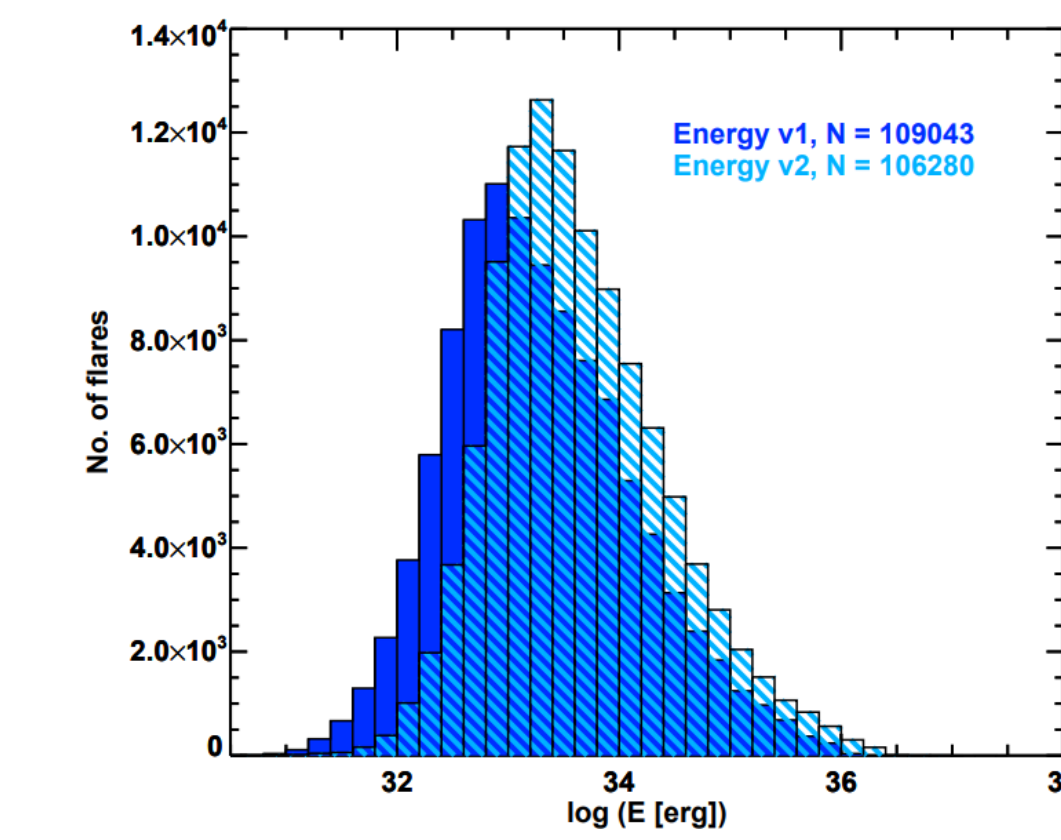


Figure 5: Distribution of flare energies estimated using methods based on Shibayama et al. (2013) (dark blue) and based on Kovari et al. (2007) (light blue).

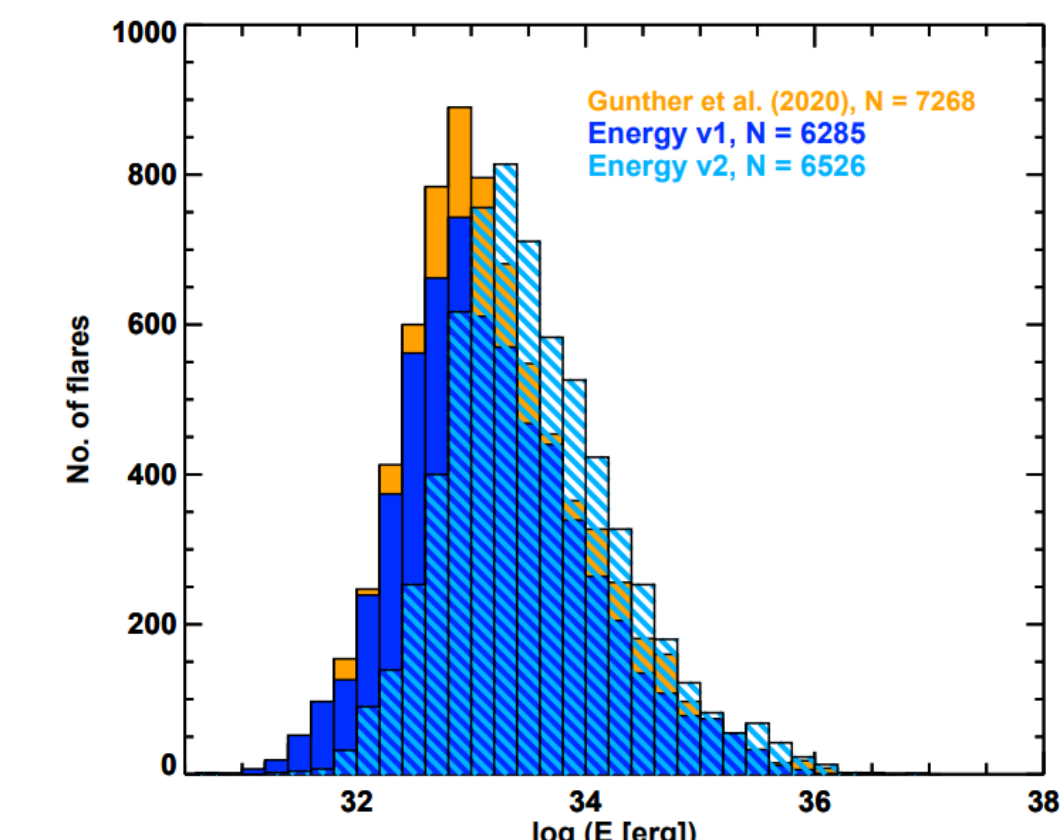


Figure 6: Distribution of flare energies from S01-S02 estimated using methods based on Shibayama et al. (2013) (dark blue) and based on Kovari et al. (2007) (light blue) and the comparison with Günther et al. (2020) (orange).

The Table 1 presents information about the stars with the flares of the highest energies found by our software. The energies was estimated using method based on Shibayama et al. (2013) (Energy v1) and Kovari et al. (2007) (Energy v2). The most energetic events have energy greater than 5×10^{35} erg. We limited our analysis only to stars with radius smaller than $2 R_{\odot}$ due to overvaluation of flares energy for stars with too large estimated radius values. Assuming that the bolometric energy of 10^{33} erg correspond to an X100 flare (Benz (2016)), detected events are more than X100000 flares.

Table 1. Table of the stars with the flares of the highest energies

TIC	Name	Energy v1 [erg]	Energy v2 [erg]	Spectral type	T_{eff} [K]	Radius [R_{\odot}]
TIC175305230	CI* NGC 2451 AR 52	9.07e+35	2.12e+36	G8V	5419	1.1
TIC468191285	LEHPM 4131	8.42e+35	1.88e+36	G9Ve	4966	0.9
TIC326092524	CD-26 332	8.41e+35	1.80e+36	G3V	5729	0.9
TIC420137030	TYC 4456-307-1	8.06e+35	1.86e+36	G0V	5935	1.1
TIC50656379	2MASS J05292131-0028357	7.76e+35	1.55e+36	M1V	3681	1.0
TIC50897755	CVSO 119	6.87e+35	1.25e+36	K7	4045	1.2
TIC81100117	2MASS J08104428-4727558	6.14e+35	1.45e+36	K3V	4885	0.8
TIC232036408	TYC 7621-604-1	5.86e+35	-	G3V	5717	1.1

REFERENCES

- [1] Benz, A. 2016, Living Reviews in Solar Physics, 14
- [2] Castelli, F., Kurucz, R. L. 2004, arXiv:astro-ph/0405087
- [3] Davenport, J. R. A., Hawley, S. L., Hebb, L., et al. 2014, The Astrophysical Journal, 797, 122
- [4] Doyle, L., Ramsay, G., Doyle, J. G. 2020, MNRAS, 494, 359
- [5] Feinstein, A., Montet, B., Ansdell, M. 2020, The Journal of Open Source Software, 5, 2347
- [6] Günther, M. N., Zhan, Z., Seager, S., et al. 2020, AJ, 159, 60
- [7] Hawley, S. L., Fisher, G. H. 1992, ApJS, 78, 565
- [8] Howard, W. S., Corbett, H., Law, N. M., et al. 2019, ApJ, 881, 9
- [9] Kovari, Z., Vilardell, F., Ribas, I., et al. 2007, Astronomische Nachrichten, 328, 904
- [10] Lacy, C. H., Moffett, T. J., Evans, D. S. 1976, ApJS, 30, 85
- [11] Maehara, H., Notsu, Y., Namekata, K., et al. 2020, Publications of the Astronomical Society of Japan, 73
- [12] Mochnacki, S. W., Zirin, H. 1980, ApJL, 239, L27
- [13] Shibayama, T., Maehara, H., Notsu, S., et al. 2013, ApJS, 209, 5